JOC The Journal of Organic Chemistry

Article

pubs.acs.org/joc

Effect of Substituents on the Structure, Stability, and π-Dimerization of Dithienylpyrrole Radical Cations

Tohru Nishinaga,* Takuya Kageyama, Masahide Koizumi, Kyoko Ando, Masayoshi Takase, and Masahiko Iyoda

Department of Chemistry, Graduate School of Science and Engineering, Tokyo Metropolitan University, Hachioji, Tokyo 192-0397, Japan

Supporting Information

ABSTRACT: A series of 2,5-di(2-thienyl)-*N*-methylpyrrole derivatives **1a**−**1d** with methylthio end-capping groups and electron-donating substituents at the 3-position of the thiophene rings was synthesized, and the effects of the substituents on the structure, stability, and π-dimerization ability of the radical cation were investigated using UV−vis−NIR and electron spin resonance spectra and density functional theory (DFT) calculations. Among the electron-donating methyl, methoxy, and methylthio substituents, the methoxy derivative **1c** gave the most stable radical cation, which persisted in dichloromethane at room temperature under nitrogen for several hours without any apparent decomposition. In addition, $\mathbf{1c}^{\bullet+}$ had the largest π-dimerization enthalpy among $\mathbf{1a}^{\bullet+}$−$\mathbf{1d}^{\bullet+}$. DFT calculations with the M06-2X method revealed that methyl and methylthio derivatives $\mathbf{1b}^{\bullet+}$ and $\mathbf{1d}^{\bullet+}$ as well as $\mathbf{1c}^{\bullet+}$ adopt a cis−cis conformation, in contrast to the trans−trans conformer of unsubstituted $\mathbf{1a}^{\bullet+}$, while the π-dimers of all of these compounds were shown to have a cis−cis conformation. On the basis of further detailed analyses, the preformed cis−cis conformation and the weaker intramolecular and intermolecular steric repulsions were considered to explain why $\mathbf{1c}^{\bullet+}$ has the largest π-dimerization enthalpy.

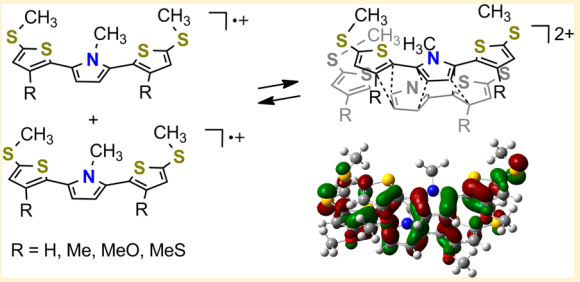

INTRODUCTION

The design and synthesis of various π-conjugated oligomers has been intensively investigated over the last few decades for use as models of the corresponding π-conjugated polymers and as part of the development of novel functional materials.[1] The use of five-membered heteroaromatics as the repeating unit of the π-conjugated oligomers is advantageous, because these oligomers exhibit better environmental stability with more effective π-conjugation due to the lower level of steric repulsion between neighboring units in planar conformations than in oligomers composed of six-membered aromatics. Among five-membered heteroaromatics, thiophene is the most commonly used component for linear oligomers, partly because of the synthetic availability of various stable derivatives.[2] Pyrrole, which has a better donor ability, is also an attractive component used in polypyrroles.[3] Nevertheless, in contrast to the plentiful examples of oligothiophenes,[1c] fewer examples of linear oligopyrroles are available in the literature, in part due to the limited synthetic access.[4−6] Thus, a pyrrole unit is often combined with thiophene rings in oligomer chemistry.[7−15]

The cationic species of π-conjugated oligomers serve as models of the corresponding conducting polymers in the p-doped state,[1a] in which electron-deficient holes play a critical role as the charge carriers. However, in general, the radical cations of shorter oligomers are highly reactive and give polymers as in the synthesis of π-conjugated polymers by electropolymerization.[16] Structural modifications with electron-donating amino,[17] alkoxy,[18−21] and arylthio or alkylthio[20−22] substituents or the annelation of bicyclo[2.2.2]octene frameworks[23,24] have been shown to be effective in stabilizing these shorter cationic oligomers. When persistent radical cations of oligomers have an open site for intermolecular interactions, face-to-face dimers (π-dimers) could be formed at higher concentrations and/or lower temperatures.[24a] It has been noted that such an intermolecular interaction between radical cations could be an alternative to the bipolaron model for conducting polymers.[25] In addition, there is growing interest in the structure and properties of the π-dimers of various persistent radicals. The interaction between the two monomers in the π-dimer is referred to as a two-electron multicenter bond.[26] Additionally, the reversible bond formation and dissociation of π-dimers have recently been employed to control the mechanical motion within molecules.[27−29]

In our previous study, we demonstrated that the biradical character of dications was enhanced in a thiophene−pyrrole mixed oligomer consisting of nine units relative to non-athiophene.[15b] If each radical moiety in the biradicals forms an intermolecular π-dimer in a slipped-stack manner, the resulting supramolecular polymer is expected to function as a conductive molecular wire. However, the moderate stability of the dication of the thiophene−pyrrole oligomers in CH_2Cl_2 solution

Received: July 5, 2013
Published: August 19, 2013

dx.doi.org/10.1021/jo401453s | J. Org. Chem. 2013, 78, 9205−9213

hampered further investigation. To realize such a system, it is necessary to synthesize a more stable radical cation unit composed of short oligomers of five-membered heteroaromatics without sterically demanding substituents. As one candidate, we designed 2,5-bis[5-(methylthio)-2-thienyl]-*N*-methylpyrrole **1** with various electron-donating substituents at the 3-position of the thienyl moiety. The electron-donating substituents at the 3-position of the thiophene ring would be effective for stabilizing the radical cation state[18b] due to the protection of the carbon atom with a relatively high spin density.[9a] Quite recently, we also successfully performed a detailed analysis of the structure–π-dimerization energy relationship in oligothiophene radical cations based on the results of experiments and density functional theory (DFT) calculations.[30] In the present study, the effects of the substituent on the structure, stability, and π-dimerization capability of radical cation of **1** were investigated by both experiments and DFT calculations. To the best of our knowledge, such a substituent effect on the π-dimerization energy of radical cations has not been investigated in detail previously. From these studies, we found that the radical cation of methoxy derivative **1c** has sufficient stability and the largest π-dimerization enthalpy. Herein, we discuss the factors driving the π-dimerization based on the results of our experiments and theoretical calculations with the M06-2X method[31] that could estimate the dimerization energy better than other modified B3LYP methods.[30]

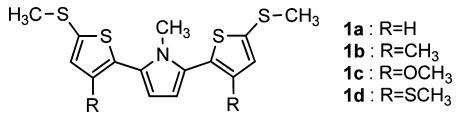

RESULTS AND DISCUSSION

Synthesis. The Paal–Knorr method using 1,4-di(2-thienyl)-1,4-butanedione is generally applied for the synthesis of 2,5-di(2-thienyl)pyrrole units,[7−15] and we also used this method in our first attempt. Dione **2a** was easily obtained by the double Friedel–Crafts reaction of succinyl chloride with thiophene.[12] Then, condensation of **2a** with methylamine gave **3a**. A previously developed procedure for the synthesis of dimethyl derivative **2b** involves the $Pb(OAc)_4$-mediated coupling of a silyl enol ether.[10] To test a new route that does not require the toxic Pb reagent, we performed a Friedel–Crafts reaction of 3-methylthiophene with chloroacetyl chloride to give **4**, followed by homocoupling using $NiBr_2(PPh_3)_2$ and activated Zn[32] to give **2b**. However, the overall yield (15%) of this route was found to be unsatisfactory. Furthermore, the attempted synthesis of dimethoxy derivative **2c** failed due to the difficulty of the Friedel–Crafts acylation of 3-methoxythiophene at the 2-position. Instead, we found a more convenient route for **3b–d** (i.e., the cross-coupling of 2-halothiophene derivatives **5** with 2,5-distannyl-*N*-methylpyrrole).[33] Thus, dimethyl derivative **3b**, dimethoxy derivative **3c**, and bis-methylthio derivative **3d** were obtained in 65%, 67%, and 43% yields, respectively. For the end-capping units used to protect the most reactive site in the radical cation state, we chose the methylthio group because of its practical balance between efficiency and accessibility. The introduction of two methylthio groups was easy via dilithiation with n-BuLi, followed by a reaction with dimethyl disulfide to give **1a–1d** (Scheme 1) in high yields.

Scheme 1. Synthesis of 1

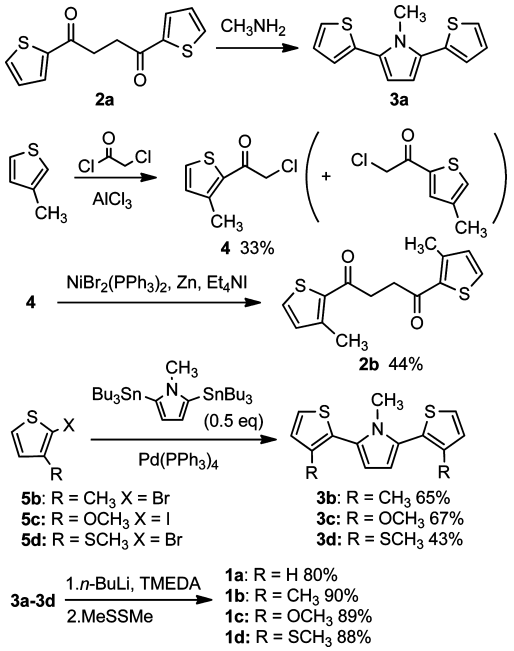

Electronic Properties of the Neutral Precursor. The electronic absorption spectra of **1** were measured in CH_2Cl_2, and the results are summarized in Table 1 together with those for methylthio end-capped terthiophene **6**, which was used as a reference compound (for the spectra, see Figure S1 in the Supporting Information). The longest absorption maximum of dithienylpyrrole **1a** was slightly blue shifted in comparison with that of terthiophene **6**. Furthermore, the introduction of substituents at the π-position of the thiophene ring in **1b–1d** caused an additional blue shift due to the twisted structure in the neutral state, as predicted by the DFT calculations (Figure S2 in the Supporting Informaiton).

Table 1. Absorption Maxima (λ_{max}) and Oxidation Potentials (E^{ox}) of 1 and 6 in CH_2Cl_2

compound	λ_{max}/nm (log ε)	$E^{ox1}{}_{1/2}$/V[a,b]	$E^{ox2}{}_{1/2}$/V[a,b]
1a	349 (5.4)	0.16	0.41
1b	313 (5.5)	0.24	0.39
1c	335 (5.3)	−0.01	0.19
1d	333 (5.3)	0.26	0.38
6	384 (5.4)	0.42	0.59

[a]Potentials vs Fc/Fc^+. [b]Concentration: 1 mM. Supporting electrolyte: 0.1 M Bu_4NPF_6.

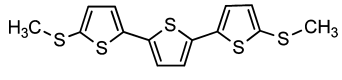

6

To study the redox behaviors of **1** and **6**, cyclic voltammetry measurements were taken, and the results are summarized in Table 1. As shown in Figure 1, reversible two-step one-electron oxidation waves were observed for all compounds, indicating that the radical cation and dication of **1** and **6** were stable under the measurement conditions. The oxidation potentials of **1** were lower than those of **6** due to the presence of a better donor pyrrole ring in **1**.[7b] Regarding the substituent effect on

dx.doi.org/10.1021/jo401453s | J. Org. Chem. 2013, 78, 9205–9213

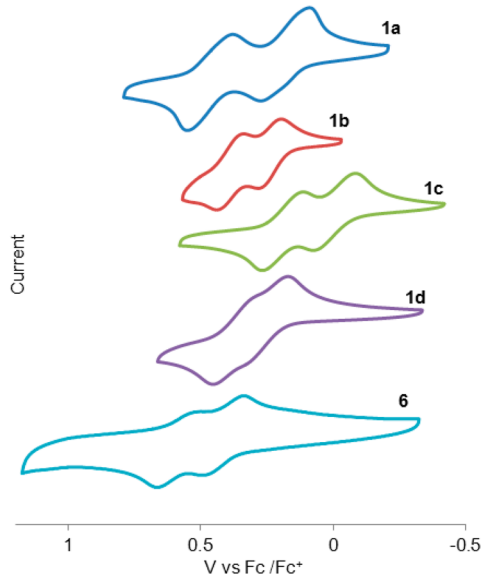

Figure 1. Cyclic voltammograms of **1a–d** and **6**.

the first oxidation potential of **1**, methyl and methylthio derivatives **1b** and **1d** were shown to have higher potentials than that of **1a**. Thus, the less effective π-conjugation due to the more twisted structure in the neutral states of **1b** and **1d** (see Figure S2 in the Supporting Information) outweighed the effect of the inductive and conjugative electron donation of the substituents. In contrast, methoxy derivative **1c** had a lower oxidation potential due to the conjugative electron donation of the oxygen atoms. As for the difference between the first and second oxidation potentials, **1b–1d** showed smaller differences than that of **1a** probably because of the reduction of on-site Coulomb repulsion brought about by the charge delocalization into the additional electron-donating substituents in **1b–1d**.

Calculated Structures of the Radical Cations. In the one-electron oxidation state, the inter-ring bonds of bithiophene[23b] and bipyrrole[19] were found to be shortened by X-ray structural analyses. This phenomenon is attributed to the significant contribution of the quinoidal resonance structure in the cationic state (Figure 2). Because of the enhanced double

Figure 2. Quinoidal resonance structures of the bithiophene radical cation.

bond character of the inter-ring bond in the radical cation state, the rotational barrier is considered to be raised, as previously observed for bithiophene and terthiophene dications.[23b]

To predict the ground state structure and the inter-ring torsional energy profiles in the one-electron oxidation state for bithiophene **7**, 2,2′-*N*,*N*′-dimethylbipyrrole **8**, and 2-(2-thienyl)-*N*-methylpyrrole **9a** and its derivatives **9b–9d** with

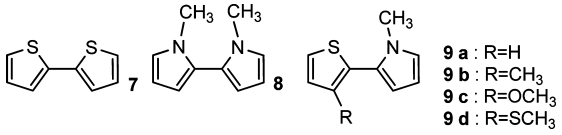

electron-donating substituents at the 3-position of the thiophene ring, DFT calculations were performed using the B3LYP and M06-2X methods with the 6-31G(d) basis set. For the inter-ring torsional energy profiles, each conformer generated upon changing the inter-ring C=C—C=C dihedral angle (θ) by 10° was optimized. Then, full optimization was performed for the cis and trans conformers. As shown in Table 2 (and Table S1 in the Supporting Information) and Figure 3

Table 2. Comparison of the Dihedral Angle (θ) and Relative Energy (ΔE) for $7^{\bullet+}$–$9^{\bullet+}$ at the B3LYP/6-31G(d) Level

compound	cis[a] θ deg/(ΔE kcal mol^{-1})	maximum[b] θ deg/(ΔE kcal mol^{-1})	trans[a] θ deg/(ΔE kcal mol^{-1})
$7^{\bullet+}$	0 (0.6)	90 (16.8)	180 (0)
$8^{\bullet+}$	31 (4.1)	80 (11.2)	157 (0)
$9a^{\bullet+}$	0 (0)	90 (14.1)	180 (0.6)
$9b^{\bullet+}$	13 (0)	90 (12.7)	144 (2.9)
$9c^{\bullet+}$	0 (0)	90 (15.4)	150 (3.2)
$9d^{\bullet+}$	23 (0)	90 (11.8)	141(3.7)

[a]Full optimized structure. [b]Least stable conformer among the optimized structures obtained upon changing the inter-ring C=C—C=C dihedral angle (θ) by 10°.

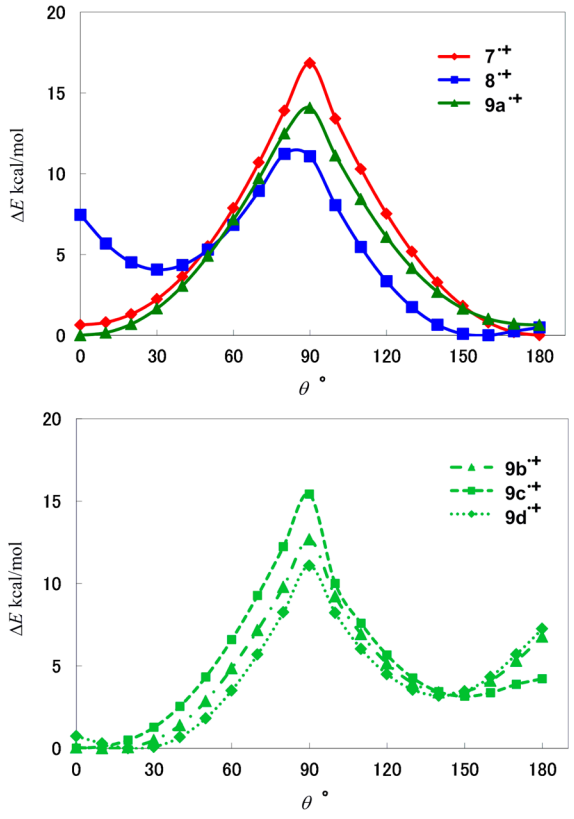

Figure 3. Inter-ring torsional energy profile for $7^{\bullet+}$–$9^{\bullet+}$ calculated at the B3LYP/6-31G(d) level.

(and Figure S3 in the Supporting Information), which present the results of the B3LYP (and M06-2X) methods, the most stable conformer for $7^{\bullet+}$ was found to be trans with θ = 180°, and the energy difference relative to the cis conformer with θ = 0° was quite small (B3LYP, 0.6 kcal mol^{-1}; M06-2X, 0.6 kcal mol^{-1}). The estimated rotational barrier was 16.8 kcal mol^{-1} (from trans conformer) with the B3LYP method (M06-2X: 17.7 kcal mol^{-1} (from trans conformer)), which is significantly greater than that for neutral bithiophene (2.7 kcal mol^{-1} (from

dx.doi.org/10.1021/jo401453s | J. Org. Chem. 2013, 78, 9205–9213

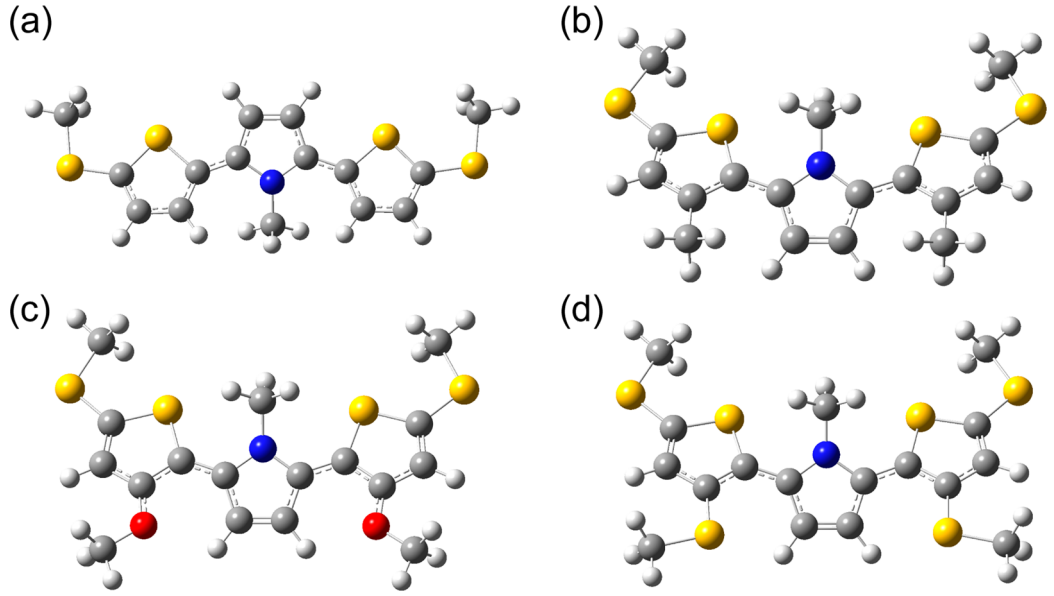

Figure 4. Optimized structures (C_s symmetry) of (a) $\mathbf{1a}^{\bullet+}$ (inter-ring C═C—C═C dihedral angle θ = 157°), (b) $\mathbf{1b}^{\bullet+}$ (θ = 26°), (c) $\mathbf{1c}^{\bullet+}$ (θ = 17°), and (d) $\mathbf{1d}^{\bullet+}$ (θ = 28°) at the B3LYP/6-31G(d) level.

trans conformer) at the B3LYP/6-31G(d) level)[34] and approximately two-thirds of that for the bithiophene dication (27.6 kcal mol^{-1} (from trans conformer)).[23b] Similarly, the energy difference between the cis and trans conformers of $\mathbf{9a}^{\bullet+}$ was found to be small, and the presence of a relatively large rotational barrier (B3LYP, 14.1 kcal mol^{-1} (from cis conformer); M06-2X, 16.2 kcal mol^{-1} (from cis conformer)) was also shown. The most stable conformer for $\mathbf{8}^{\bullet+}$ was trans (B3LYP, θ = 157°; M06-2X, θ = 157°), and the energy difference relative to the cis conformer (B3LYP, θ = 31°; M06-2X, θ = 31°) was 4.1 kcal mol^{-1} with the B3LYP method (M06-2X, 3.8 kcal mol^{-1}). The instability of the cis conformers of $\mathbf{8}^{\bullet+}$ was ascribed to the steric repulsion between the *N*-methyl groups.

For $\mathbf{9b}^{\bullet+}$–$\mathbf{9d}^{\bullet+}$, levels of steric repulsion between the *N*-methyl group and the substituents at the 3-position of the thiophene ring similar to those observed in $\mathbf{8}^{\bullet+}$ are considered to exist. In the case of $\mathbf{9b}^{\bullet+}$–$\mathbf{9d}^{\bullet+}$, however, it is not the cis but the trans conformers that are destabilized by the steric repulsion, and as a result, the cis conformers are expected to be more stable. As shown in Figure 3 and Table 2, the most stable conformers for $\mathbf{9b}^{\bullet+}$–$\mathbf{9d}^{\bullet+}$ were found to be cis, and the energy differences relative to the destabilized trans conformers were calculated to be 3–4 kcal mol^{-1}. The rotational barriers of $\mathbf{9b}^{\bullet+}$ and $\mathbf{9d}^{\bullet+}$ were found to be smaller than that of $\mathbf{9a}^{\bullet+}$, most likely due to the destabilization of the fully planar cis conformer caused by steric repulsion between the substituent on the thienyl ring and the adjacent pyrrole ring. In contrast, the barrier for $\mathbf{9c}^{\bullet+}$ is slightly higher than that of $\mathbf{9a}^{\bullet+}$, suggesting that the methoxy substituent enhances the double bond character of the inter-ring bond. In accordance with this explanation, the calculated bond length in $\mathbf{9c}^{\bullet+}$(θ = 0°) (B3LYP, 1.408 Å; M06-2X, 1.404 Å) is slightly shorter than that in $\mathbf{9a}^{\bullet+}$(θ = 0°) (B3LYP, 1.410 Å; M06-2X, 1.406 Å).

According to these theoretical predictions, dithienylpyrroles **1b**–**1d** are novel π-conjugated oligomers of five-membered heteroaromatics that have a cis–cis conformation in the one-electron oxidation state. As shown in Figure 4 (and Figure S4 in the Supporting Information), the optimized structures of $\mathbf{1b}^{\bullet+}$–$\mathbf{1d}^{\bullet+}$ at the B3LYP/6-31G(d) and M06-2X/6-31G(d) levels were confirmed to have cis–cis conformations, in contrast to the trans–trans conformation of $\mathbf{1a}^{\bullet+}$. In the calculated ground state structures, there were some twists in the π-systems due to the repulsion between the methyl group in the pyrrole ring and the thiophene units. The inter-ring C═C—C═C dihedral angles θ for $\mathbf{1a}^{\bullet+}$–$\mathbf{1d}^{\bullet+}$ at the B3LYP/6-31G(d) level (and the M06-2X/6-31G(d) level) were 157° (157°), 26° (24°), 17° (16°), and 28° (27°), respectively. The smaller dihedral angle in $\mathbf{1c}^{\bullet+}$ is due to the enhanced double bond character in the inter-ring bond, as described above. The results of the DFT calculations of $\mathbf{3b}^{\bullet+}$ have been reported previously, although the calculations were only performed for the trans–trans conformer.[10] The present results indicate that the cis–cis conformer is more stable than the trans–trans conformer for $\mathbf{3b}^{\bullet+}$ as well as $\mathbf{1b}^{\bullet+}$.

Synthesis and Stability of the Radical Cations. The radical cation salts of **1a**, **1c**, and **1d** were generated with nitrosonium hexafluoroantimonate ($NOSbF_6$) in CH_2Cl_2 under sonication at room temperature. Then, hexane was added to the dark blue solution to precipitate the radical cation salts. The precipitates were washed with hexane several times. Elemental analyses of these salts showed that $\mathbf{1a}^{\bullet+}SbF_6^-$, $\mathbf{1c}^{\bullet+}SbF_6^-$, and $\mathbf{1d}^{\bullet+}SbF_6^-$ were obtained with good purities (>94%). In the case of **1b**, one-electron oxidation with $NOSbF_6$ did not complete; this reaction might stop primarily at the formation of the nitrosonium complex judging from the different reddish color present after a faint blue color. Thus, for the generation of a radical cation from **1b**, silver hexafluoroantimonate ($AgSbF_6$) was used instead.

The UV–vis–NIR spectra of $\mathbf{1a}^{\bullet+}$–$\mathbf{1d}^{\bullet+}$ were measured in CH_2Cl_2 under nitrogen at room temperature. The observed absorption bands are summarized in Table 3 and were compared with the calculated bands (time-dependent density functional theory (TD-DFT) calculations at the M06-2X/6-31G(d) levels) for the cis–cis and trans–trans conformers. The polarizable continuum model (PCM) was combined with TD-DFT to compute the spectra in CH_2Cl_2. As shown in Figure 5, the calculated absorption bands reproduced the features of the

dx.doi.org/10.1021/jo401453s | J. Org. Chem. 2013, 78, 9205–9213

Table 3. Observed and Calculated Absorption Bands (λ) for the Radical Cations $1a^{\bullet+}$–$1d^{\bullet+}$ and $6^{\bullet+}$ and Their π-Dimers and Differences in the Total Energies of the Radical Cations between Cis–Cis and Trans–Trans Conformers (E_{tt}–E_{cc}) in CH_2Cl_2

	radical cation			π-dimer	
compound	$\lambda_{(exp)}$/nm	$\lambda_{(calcd)}$/nm	$E_{tt} - E_{cc}$/ kcal mol^{-1}	$\lambda_{(exp)}$/nm	$\lambda_{(calcd)}$/nm
$1a^{\bullet+}$	577, 947	437, 459, 851[a,b]	−1.2	492, 760, 935	377, 620, 825[b]
$1b^{\bullet+}$	497, 567, 1000	441, 864[b,c]	1.0	506, 822, 1015	392, 647, 923[b]
$1c^{\bullet+}$	570, 878	465, 720[b,c]	0.8	498, 721, 951	392, 396, 561, 857[b]
$1d^{\bullet+}$	596, 1033	464, 887[b,c]	1.8	548, 951, 1340	411, 636, 1013[b]
$6^{\bullet+}$	655, 1100[d]	528, 923[b,c]	−0.9	524, 838, 1094[d]	413, 664, 851[b]

[a]Calculated with the trans–trans conformer. [b]Calculated at the TD-M06-2X/6-31G(d) level with PCM (CH_2Cl_2). Absorption maximum with oscillator strength more than 0.29. [c]Calculated with the cis–cis conformer. [d]Reference 22. Measured in CH_3CN.

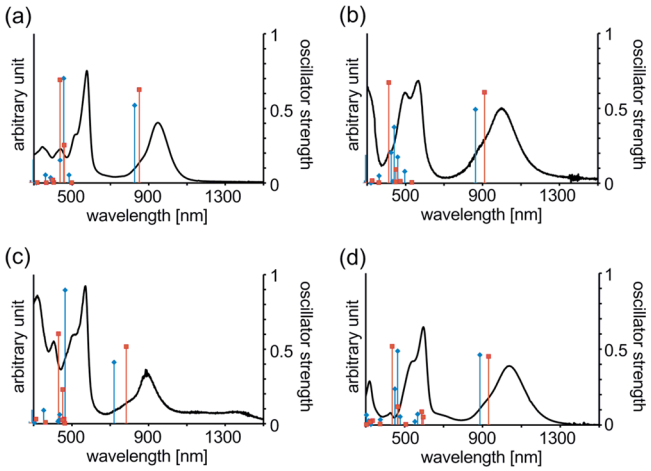

Figure 5. Absorption spectra of (a) $1a^{\bullet+}$, (b) $1b^{\bullet+}$, (c) $1c^{\bullet+}$, and (d) $1d^{\bullet+}$. The results of the TD-DFT calculations at the TD-M06-2X/6-31G(d) level with PCM (CH_2Cl_2) are also depicted as bar graphs. The blue and red bars are for the cis–cis and trans–trans conformers, respectively.

experimental spectra, although the calculated transition energies were somewhat overestimated. A similar discrepancy (100–200 nm) was also observed for a series of oligothiophene radical cations in our previous study.[30] The spectra are composed of two primary bands, as is the spectrum of $6^{\bullet+}$.[22] The bands in the longer and shorter wavelength regions were assigned as the HOMO–SOMO and SOMO–LUMO transition, respectively. For $1a^{\bullet+}$ and $6^{\bullet+}$, the calculations indicate that the trans–trans conformers are more stable than the cis–cis conformers by approximately 1 kcal mol^{-1} at the M06-2X/6-31G(d) level with PCM, suggesting that the spectra primarily reflect the absorption bands of the trans–trans conformers. In contrast, the cis–cis conformers of $1b^{\bullet+}$ (1.02 kcal mol^{-1}), $1c^{\bullet+}$ (0.75 kcal mol^{-1}), and $1d^{\bullet+}$ (1.80 kcal mol^{-1}) were more stable than the corresponding trans–trans conformers in CH_2Cl_2, as observed in the calculations in vacuo (vide supra). For $1a^{\bullet+}$, $1b^{\bullet+}$, and $1d^{\bullet+}$, the oscillator strengths of the two bands in the cis–cis and trans–trans conformers were predicted to be similar (Figure 5a,b,d). In contrast, the apparent difference in the oscillator strength between the two bands for the cis–cis conformer of $1c^{\bullet+}$ was predicted, whereas this difference was calculated to be small for the trans–trans conformer (Figure 5c). The experimental spectrum of $1c^{\bullet+}$ appeared to be similar to the calculated spectrum of cis–cis conformer, which may suggest that $1c^{\bullet+}$ has a cis–cis conformation in solution.

To assess the stability of the radical cations $1a^{\bullet+}SbF_6^-$–$1d^{\bullet+}SbF_6^-$, the decomposition rate in CH_2Cl_2 under nitrogen at room temperature was analyzed using the second absorption band at approximately 600 nm. The radical cation $6^{\bullet+}SbF_6^-$, which was generated with $NOSbF_6$, was also analyzed. As shown in Figure 6, radical cations $1b^{\bullet+}$–$1d^{\bullet+}$ were more stable

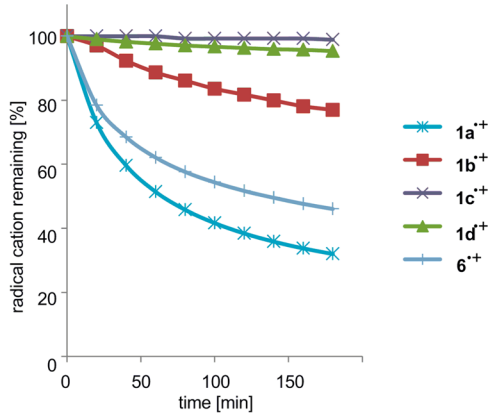

Figure 6. Decomposition rate of $1a^{\bullet+}SbF_6^-$–$1d^{\bullet+}SbF_6^-$ and $6^{\bullet+}SbF_6^-$ in CH_2Cl_2 under nitrogen at room temperature.

than $1a^{\bullet+}$ and terthiophene $6^{\bullet+}$ due to the presence of the electron-donating substituents at the 3-position of the thiophene ring, while reduction to the corresponding neutral species appeared to mainly occur in the decomposition processes (see Figure S5 in the Supporting Information). Among $1b^{\bullet+}$–$1d^{\bullet+}$, the methoxy and methylthio derivatives $1c^{\bullet+}$ and $1d^{\bullet+}$ were further stabilized, and only a small amount of the radical cation had decomposed after 3 h. Thus, conjugative electron donation at the 3-position of the thiophene carbon, which has a relatively high spin density, is more effective for stabilizing the radical cations than electron donation by the simple methyl group.

π-Dimer Formation. The electron spin resonance (ESR) spectra of $1a^{\bullet+}$–$1d^{\bullet+}$ were measured in CH_2Cl_2 at room temperature. As shown in Figure 7, all of the radical cation salts exhibited ESR signals at room temperature, and the intensity of the signals decreased as the temperature decreased. These results indicate that the doublet radical cations formed singlet species at lower temperatures.

The equilibrium shift to π-dimer formation by the radical cations (Scheme 2) in CH_2Cl_2 solution was studied using variable temperature UV–vis–NIR spectra. Spectral changes similar to those of other oligothiophene radical cations were observed for $1a^{\bullet+}$–$1d^{\bullet+}$ upon lowering the temperature. As shown in Figure 8 (and Figure S6 in the Supporting Information), the two absorption bands assigned to radical cation monomers showed hypsochromic shifts upon π-dimer formation, and a new band assigned to the HOMO–LUMO transition of the π-dimer arose in the longer wavelength region. These diagnostic absorption bands for π-dimer formation[18b] are

dx.doi.org/10.1021/jo401453s | J. Org. Chem. 2013, 78, 9205–9213

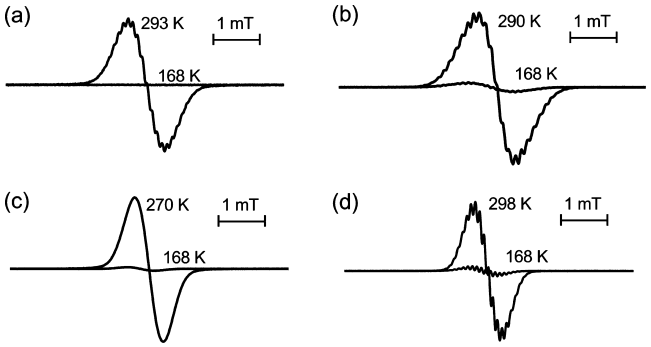

Figure 7. ESR spectra of (a) $\mathbf{1a}^{\bullet+}$ (0.1 mM), (b) $\mathbf{1b}^{\bullet+}$ (1.5 mM), (c) $\mathbf{1c}^{\bullet+}$(0.1 mM), and (d) $\mathbf{1d}^{\bullet+}$(0.4 mM).

Scheme 2. π-Dimer Formation of Radical Cation of 1

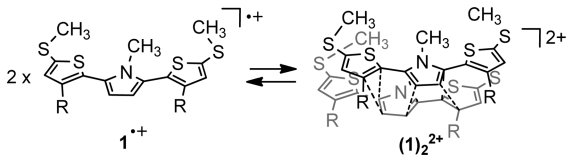

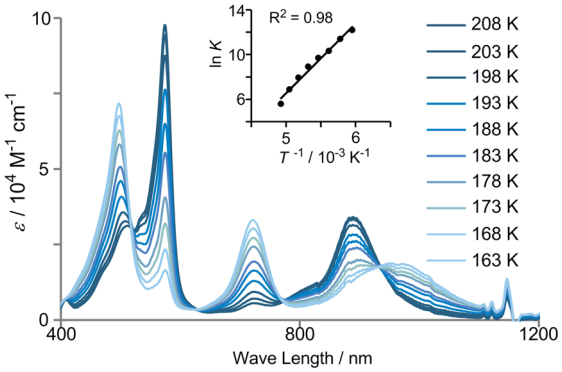

Figure 8. UV–vis–NIR spectra of $\mathbf{1c}^{\bullet+}$ (3.11×10^{-5} M) at various temperatures.

also summarized in Table 3. From the change in the second absorption bands of the π-dimer in these absorption spectra, the equilibrium constant for the dimerization process at each temperature was estimated given that the π-dimer formation was the only ongoing reaction judging from the appearance of isosbestic points. Then, the thermodynamic parameters $\Delta H_{\mathrm{dim(exp)}}$ and $\Delta S_{\mathrm{dim(exp)}}$ were obtained with a van't Hoff plot and are summarized in Table 4.

The comparison of the $\Delta H_{\mathrm{dim(exp)}}$ of $\mathbf{1a}^{\bullet+}$ with that of the methyl end-capped terthiophene (−10 kcal mol^{-1})[35] indicated that the possible steric repulsion between the methyl groups of the pyrrole ring was negligible. Among $\mathbf{1a}^{\bullet+}$–$\mathbf{1d}^{\bullet+}$, methoxy derivative $\mathbf{1c}^{\bullet+}$ was shown to have the largest dimerization enthalpy. In a previous study, the steric repulsion of the alkyl substituent in the β-position of thiophene caused the repression of the π-dimerization of oligothiophenes.[36] A similar repression was also observed for $\mathbf{1b}^{\bullet+}$, and a higher concentration and lower temperatures were required to observe the dimerization (Figure S6 in the Supporting Information). Similarly, the dimerization process for $\mathbf{1d}^{\bullet+}$ was further repressed. In contrast, the dimerization process for $\mathbf{1c}^{\bullet+}$ was observed even in a lower concentration and at higher temperatures. Thus, only the methoxy group was found to be a favorable substituent for the dimerization.

To provide insight into these results, DFT calculations were performed. We chose the M06-2X method with the 6-31G(d) basis set because this method reproduced the X-ray structure of the π-dimer of the bicyclo[2.2.2]octene end-capped terthiophene radical cation very well and also qualitatively reproduced the order of the π-dimerization enthalpy for the series of bicyclo[2.2.2]octene-annulated oligothiophenes.[30] In contrast, the B3LYP method failed to reproduce the structure of the dimer and related modified B3LYP methods did not give reasonable dimerization energies.[30] As reported previously, the most stable π-dimer structure for oligothiophene radical cations without the annulation at the β-position is the face-to-face dimer of primarily cis-connected banana-shaped conformers with slipped-stack structures along the long axis. This structure is the result of the balance between the maximization of the bonding interaction of the SOMO of the radical cation and the minimization of the intermolecular repulsion of the larger sulfur atoms. Similarly, the most stable structures of π-dimer $(\mathbf{1a})_2^{2+}$ and $(\mathbf{6})_2^{2+}$ (Figure S7 in the Supporting Information) among several optimized structures were found to be face-to-face dimers of cis–cis conformers. The optimized structures of $(\mathbf{1b})_2^{2+}$–$(\mathbf{1d})_2^{2+}$ also looked similar, with the preformed cis–cis conformations with some twisted structures in the monomer states becoming flat upon π-dimerization (Figure 9 and Figure S7 in the Supporting Information). The shortest intermolecular C–C contacts ($(\mathbf{1a})_2^{2+}$, 2.961 Å ($C_{\beta(\mathrm{thiophene})}$–$C_{\beta(\mathrm{pyrrole})}$); $(\mathbf{1b})_2^{2+}$, 3.026 Å ($C_{\beta(\mathrm{thiophene})}$–$C_{\beta(\mathrm{pyrrole})}$); $(\mathbf{1c})_2^{2+}$, 2.968 Å ($C_{\beta(\mathrm{thiophene})}$–$C_{\beta(\mathrm{pyrrole})}$); $(\mathbf{1d})_2^{2+}$, 3.008 Å ($C_{\beta(\mathrm{thiophene})}$–$C_{\beta(\mathrm{thiophene})}$)) were less than the sum of the van der Waals radius of carbon (3.4 Å) due to the SOMO–SOMO interaction, as shown in the representative plot of the HOMO of $(\mathbf{1c})_2^{2+}$ (Figure 9c). The longer C–C contacts in $(\mathbf{1b})_2^{2+}$ and $(\mathbf{1d})_2^{2+}$ than in $(\mathbf{1a})_2^{2+}$ reflect steric repulsion due to the methyl or methylthio substituents, whereas the comparable lengths for $(\mathbf{1a})_2^{2+}$ and $(\mathbf{1c})_2^{2+}$ indicate that such steric repulsion is negligible for the methoxy group. These structural features were essentially the same as those without PCM.

Table 4. Dimerization Enthalpy (ΔH_{dim}/kcal mol^{-1}) and Entropy (ΔS_{dim}/cal K^{-1} mol^{-1}), Calculated π-Dimerization Energies (ΔE_{dim}), SOMO–SOMO Interactions ($\Delta E_{\mathrm{S-S(calcd)}}$), Differences in van der Waals Force (ΔE_{vdW}), Solvation Energies (ΔE_{sol}), and Intradimer Coulomb Repulsion Energies (ΔE_{Coul})

compound	$\Delta H_{\mathrm{dim(exp)}}{}^{a}$	$\Delta S_{\mathrm{dim(exp)}}{}^{a}$	$\Delta H_{\mathrm{dim(calcd)}}$	ΔE_{dim}	$\Delta E_{\mathrm{S-S(exp)}}$	$\Delta E_{\mathrm{S-S(calcd)}}$	ΔE_{vdW}	ΔE_{sol}	ΔE_{Coul}
1a	−11.1	−35	−14.6	−16.2	−30.6	−34.7	3.7	−39.0	53.8
1b	−11.8	−60	−11.1	−13.8	−28.2	−31.0	−0.8	−37.0	55.0
1c	−12.2	−45	−19.6	−20.9	−30.1	−33.4	−5.9	−35.8	54.1
1d	−9.7	−43	−11.0	−13.3	−21.3	−28.2	−0.4	−34.2	49.5

[a]Experimental errors were within ±1 kcal mol^{-1} and ±6 cal K^{-1} mol^{-1}.

dx.doi.org/10.1021/jo401453s | J. Org. Chem. 2013, 78, 9205–9213

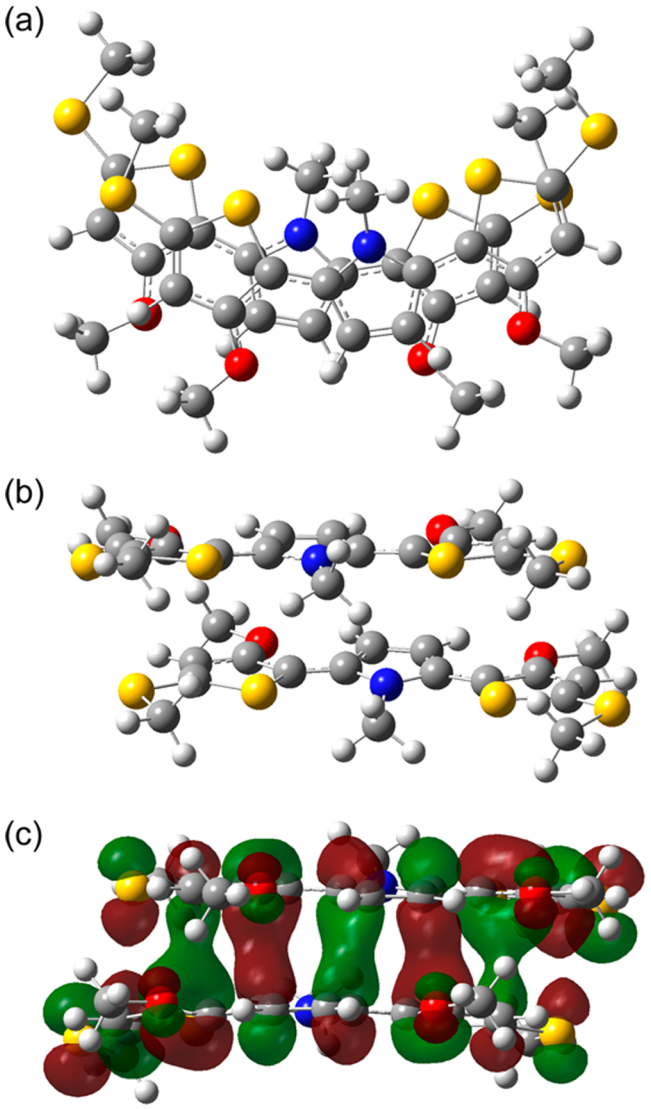

Figure 9. (a) Top and (b) side views and (c) HOMO of the optimized structures of π-dimers $(\mathbf{1c})_2^{2+}$ at the M06-2X/6-31G(d) level with PCM (CH_2Cl_2).

The dimerization enthalpy $\Delta H_{\mathrm{dim(calcd)}}$ and the dimerization energy ΔE_{dim} (i.e., the difference in the total energy) were estimated using the following equations:

$$\Delta E_{\mathrm{dim}} = E_{\pi\text{-dimer}} - 2 \times E_{\mathrm{radical\,cation}}$$

$$\Delta H_{\mathrm{dim(calcd)}} = H_{\pi\text{-dimer}} - 2 \times H_{\mathrm{radical\,cation}}$$

The $\Delta H_{\mathrm{dim(calcd)}}$ values qualitatively reproduced the order of $\Delta H_{\mathrm{dim(exp)}}$ (Table 4) with overestimation similar to that observed in our previous study. Then, we further investigated which factors are important in the substituent effect on π-dimerization. For this purpose, we divided ΔE_{dim} into the following four factors according to our previous study:[30] (1) SOMO−SOMO interactions ($\Delta E_{\mathrm{S-S}}$), (2) van der Waals forces (ΔE_{vdW}), (3) solvation (ΔE_{sol}), and (4) Coulomb repulsion (ΔE_{Coul}). The $\Delta E_{\mathrm{S-S}}$ was estimated from the HOMO−LUMO gap of the π-dimer (i.e., $E_{\mathrm{H-L}}$), which was calculated from the HOMO−LUMO transition energy obtained by the TD-M06-2X/6-31G(d) method.

$$\Delta E_{\mathrm{S-S}} = -E_{\mathrm{H-L}} \quad (1)$$

The ΔE_{vdW} was estimated using the total energies obtained from the single-point calculations of the neutral molecule in the radical cation and π-dimer geometries (i.e., $E_{\mathrm{n@rc}}$ and $E_{\mathrm{n@pd}}$, respectively) and was calculated by subtracting the $E_{\mathrm{n@rc}}$ from $E_{\mathrm{n@pd}}$ twice (eq 2):

$$\Delta E_{\mathrm{vdW}} = E_{\mathrm{n@pd}} - 2 \times E_{\mathrm{n@rc}} \quad (2)$$

The stabilization energies upon π-dimerization by solvation (i.e., ΔE_{sol}), were estimated from eq 3, where $E_{\mathrm{sol\,mon}}$ and $E_{\mathrm{sol\,dim}}$ represent the solvation energies of the monomer and π-dimer, respectively, obtained from the differences in the calculated total energy of the radical cation monomers in vacuo and in dichloromethane:

$$\Delta E_{\mathrm{sol}} = E_{\mathrm{sol\,dim}} - 2 \times E_{\mathrm{sol\,mon}} \quad (3)$$

Then, if we assume that the four factors dominate the π-dimerization process, the change in the π-dimerization energy ΔE_{dim} can be expressed as eq 4:

$$\Delta E_{\mathrm{dim}} = \Delta E_{\mathrm{S-S}} + \Delta E_{\mathrm{vdW}} + \Delta E_{\mathrm{sol}} + \Delta E_{\mathrm{Coul}} \quad (4)$$

Because ΔE_{dim}, $\Delta E_{\mathrm{S-S}}$, ΔE_{vdW}, and ΔE_{sol} were already obtained, ΔE_{Coul} was simply calculated from eq 4.

As described above, the methoxy substituents increased the dimerization enthalpy in both the experimental and calculated results, whereas the methyl and methylthio substituents had the opposite effects. For **1a** and **1c**, both $\Delta E_{\mathrm{S-S(calcd)}}$ and $\Delta E_{\mathrm{S-S(exp)}}$ had similar values, indicating that the SOMO−SOMO interactions in $(\mathbf{1a})_2^{2+}$ and $(\mathbf{1c})_2^{2+}$ are comparable. It is worth noting that the calculated intermolecular atomic contacts for $(\mathbf{1a})_2^{2+}$ and $(\mathbf{1c})_2^{2+}$ also gave similar values, suggesting that the bonding SOMO−SOMO interactions are related to the bond length. In contrast, the $-\Delta E_{\mathrm{sol}}$ for **1c** was shown to be smaller than that of **1a** because the efficient charge delocalization into the methoxy substituents causes a weaker ion−solvent interaction for $(\mathbf{1c})_2^{2+}$ than for $(\mathbf{1a})_2^{2+}$ with a denser charge distribution. Therefore, the primary reason for the larger dimerization energy of **1c** is the difference in ΔE_{vdW}. The positive ΔE_{vdW} for **1a** is considered to be primarily due to the unfavorable conformational change from a trans−trans to cis−cis structure upon π-dimerization, whereas the ΔE_{vdW} for **1c** was −5.9 kcal mol^{-1} due to the preformed cis−cis structure in the monomer state. In the case of **1b** and **1d**, ΔE_{vdW} was smaller than that of **1c** despite the similar preformed cis−cis structure. This result is considered to reflect the greater steric repulsion between the methyl or methylthio groups and the β-proton of the adjacent pyrrole ring in the cis conformer, as shown in Figure 3. In addition, the $\Delta E_{\mathrm{S-S}}$ values of **1b** and **1d** were found to be smaller than that of **1c** due to the longer bond length, which was primarily due to intermolecular steric repulsion.[37] These intramolecular and intermolecular steric repulsions caused by the methyl and methylthio substituents resulted in the smaller dimerization enthalpies of **1b** and **1d**.

CONCLUSION

As part of our research on how to obtain a stable radical cation unit composed of a small number of five-membered heteroaromatics, we investigated the effect of electron-donating substituents at the 3-position of the thiophene rings in 2,5-di(2-thienyl)-*N*-methylpyrrole on the structure, stability, and π-dimerization ability of the radical cation. Among methyl, methoxy, and methylthio groups, the methoxy group (derivative **1c**) gave the stable radical cation in dichloro-

dx.doi.org/10.1021/jo401453s | J. Org. Chem. 2013, 78, 9205−9213

methane at room temperature under nitrogen, persisting for several hours. Furthermore, $\mathbf{1c}^{\bullet+}$ had the largest π-dimerization enthalpy among $\mathbf{1a}^{\bullet+}-\mathbf{1d}^{\bullet+}$. The detailed analysis using DFT calculations revealed that the preformed cis−cis conformation and the weaker intramolecular and intermolecular steric repulsions caused the efficient π-dimerization of $\mathbf{1c}^{\bullet+}$. Thus, 2,5-bis(3-methoxy-2-thienyl)-*N*-methylpyrrole is potentially useful as a new unit for π-dimer-based supramolecular chemistry, which has been of growing interest in recent years.

EXPERIMENTAL SECTION

General Information. Commercially available reagents were used as received. Solvents were distilled from relevant drying agents prior to use. 1,4-Di(2-thienyl)-1,4-butanedione (**2a**),[12] 2,5-di(2-thienyl)-*N*-methylpyrrole (**3a**),[10] 2,5-bis(tributylstannyl)-*N*-methylpyrrole,[33] 2-bromo-3-methylthiophene (**5b**),[38] 2-bromo-3-methylthiophene (**5c**),[39] 2-bromo-3-methylthiophene (**5d**),[40] and 2,5″-bis(methylthio)-5,2′:5′,2″-terthienyl (**6**)[22] were prepared according to the literature procedures.

Synthesis of 2b. To $AlCl_3$ (13.6 g, 102 mmol) suspended in hexane (45 mL) was added dropwise a hexane (15 mL) solution of 3-methylthiophene (4.15 mL, 43.0 mmol) and chloroacetyl chrolide (3.70 mL, 46.5 mmol) under N_2. The reaction mixture was refluxed overnight and then quenched with aqueous HCl. The crude mixture was washed with aqueous solution of NH_4Cl, the aqueous layer was extracted with ether, and the ethereal solution was dried over $MgSO_4$. After filtration, volatiles were removed in vacuo, and the residue was purified by column chromatography (SiO_2) with hexane−ethyl acetate (v/v = 10:1) as eluent to give **4** (2.49 g, 14.2 mmol, 33%) as yellow oil: ^{1}H NMR ($CDCl_3$) δ 7.49 (d, 1H, J = 5.0 Hz), 7.00 (d, 1H, J = 5.0 Hz), 4.55 (s, 2H), 2.60 (s, 3H).

Activated Zn (1.28 g, 19.6 mmol), $NiBr_2(PPh_3)_2$ (0.505 g, 0.68 mmol), and Et_4NI (3.37 g, 13.1 mmol) were added to a two-necked flask and dried in vacuo for 30 min. THF (10 mL) was added to the mixture and stirred for 40 min at rt. To this mixture was added a THF (5 mL) solution of **4** (2.25 g, 12.9 mmol), and the resulting mixture was stirred overnight. After filtration, the volatiles were removed from the mixture in vacuo, and the residue was purified by column chromatography (SiO_2) with hexane−ethyl acetate (v/v = 5:1) as eluent to give **2b** (0.791 g, 2.84 mmol, 44%) as colorless crystals: ^{1}H NMR ($CDCl_3$) δ 7.42 (d, 2H, J = 5.0 Hz), 6.95 (d, 2H, J = 5.0 Hz), 3.31 (s, 4H), 2.58 (s, 6H); ^{13}C NMR ($CDCl_3$) δ 192.0, 145.3, 135.6, 132.6, 129.8, 35.5, 17.0. Anal. Calcd for $C_{14}H_{14}O_2S_2$: C, 60.40; H, 5.07. Found: C, 60.11; H, 5.13.

General Procedure for 3b−3d. A mixture of 2-halothiophene **5**, 2,5-bis(tributylstannyl)-*N*-methylpyrrole (0.5 equiv), and $Pd(PPh_3)_4$ (10 mol %) was stirred in toluene under N_2 overnight at 120 °C. The resulting mixture was then allowed to cool down to room temperature and was filtered off, and the volatiles were removed from the mixture in vacuo. The residue was purified by preparative gel permeation chromotography (GPC), eluted with $CHCl_3$, and recrystallized from a mixture of dichloromethane and ethanol to afford **3**.

3b: 65% yield; colorless crystals; mp 40.6−41.5 °C; ^{1}H NMR (500 MHz) δ 7.26 (d, 2H, J = 6.3 Hz), 6.94 (d, 2H, J = 6.3 Hz), 6.27 (s, 2H), 3.35 (s, 3H), 2.20 (s, 6H); ^{13}C NMR ($CDCl_3$) δ 133.1, 129.4, 128.7, 126.4, 125.7 111.6, 32.9, 17.6; HRMS (APCI) calcd for $[C_{15}H_{15}NS_2]$ $[(M + H)^+]$ = 274.0719, found 274.0736.

3c: 67% yield; pale yellow solid; mp 81.7−83.0 °C; ^{1}H NMR (500 MHz) δ 7.21 (d, 2H, J = 5.4 Hz), 6.90 (d, 2H, J = 5.4 Hz), 6.31 (s, 2H), 3.83 (s, 6H), 3.49 (s, 3H); ^{13}C NMR ($CDCl_3$) δ 154.1, 125.5, 123.5, 116.8, 111.7, 110.8, 58.7, 32.8; HRMS (APCI) calcd for $[C_{15}H_{15}NO_2S_2]$ $[(M + H)^+]$ = 306.0617, found 306.0644.

3d: 43% yield; pale yellow solid; mp 72.5−74.5 °C; ^{1}H NMR (500 MHz) δ 7.35 (d, 2H, J = 5.4 Hz), 7.07 (d, 2H, J = 5.4 Hz), 6.35 (s, 2H), 3.47 (s, 3H), 2.37 (s, 6H); ^{13}C NMR ($CDCl_3$) δ 133.1, 129.4, 128.7, 126.4, 125.7, 111.6, 32.9, 17.6; HRMS (APCI) calcd for $[C_{15}H_{15}NS_4]$ $[(M + H)^+]$ = 338.0160, found 338.0177.

General Procedure for 1a−1d. To a THF solution of **3**, was added *n*-butyllithium (2.5 equiv) in hexane at −78 °C under N_2. After the mixture was stirred for 1 h, dimethyl disulfide (3 equiv) was added dropwise to the reaction mixture and then allowed to warm to room temperature. After the mixture was stirred overnight, water was added, and the mixture was extracted with ether and dried over Na_2SO_4. After removal of the solvent in vacuo, the reaction mixture was passed through a short column chromatography (SiO_2 deactivated with 10% water) using hexane/acetyl acetate (v/v = 25:1) as eluent. After evaporation, the residue was separated by preparative GPC eluted with toluene to give **1**.

1a: pale yellow solid; mp 101.3−102.5 °C; ^{1}H NMR ($CDCl_3$) δ 7.04 (d, 2H, J = 5 0.1 Hz), 6.90 (d, 2H, J = 5 0.1 Hz), 3.73 (s, 3H), 2.52 (s, 6H); ^{13}C NMR ($CDCl_3$) δ 137.1, 136.6, 131.4, 129.2, 125.7, 110.3, 33.7, 22.1; HRMS(APCI) calcd for $[C_{15}H_{15}NS_4]$ $[(M + H)^+]$ = 338.0160, found 338.0149. Anal. Calcd for $C_{15}H_{15}NS_4$: C, 53.37; H, 4.48; N, 4.15. Found: C, 53.65; H, 4.50; N, 4.05.

1b: yellow oil; ^{1}H NMR ($CDCl_3$) δ 6.90 (s, 2H), 6.24 (s, 2H), 3.38 (s, 3H), 2.51 (s, 6H), 2.13 (s, 6H); ^{13}C NMR ($CDCl_3$) δ 137.1, 136.4, 133.0, 130.8, 126.8, 111.0, 32.5, 21.6, 14.8; HRMS (APCI) calcd for $[C_{17}H_{19}NS_4]$ $[(M + H)^+]$ = 366.0473, found 366.0475. Anal. Calcd for $C_{17}H_{19}NS_4$: C, 55.85; H, 5.24; N, 3.83. Found: C, 56.06; H, 5.33; N, 3.70.

1c: yellow crystals; mp 77.4−78.4 °C; ^{1}H NMR ($CDCl_3$) δ 6.89 (s, 2H), 6.28 (s, 2H), 3.80 (s, 6H), 3.49 (s, 3H), 2.52(s, 6H); ^{13}C NMR ($CDCl_3$) δ 153.2, 134.8, 125.3, 120.0, 113.7, 111.0, 58.7, 32.9, 21.5; HRMS (APCI) calcd for $[C_{17}H_{19}NO_2S_4]$ $[(M + H)^+]$ = 398.0371, found 398.0376. Anal. Calcd for $C_{17}H_{19}NO_2S_4$: C, 51.35; H, 4.82; N, 3.52. Found: C, 51.36; H, 4.83; N, 3.43.

1d: pale yellow oil; ^{1}H NMR ($CDCl_3$) δ 7.00 (s, 2H), 6.33 (s, 2H), 3.49 (s, 3H), 2.53 (s, 6H), 2.35 (s, 6H); ^{13}C NMR ($CDCl_3$) δ 153.2, 134.8, 125.3, 120.0, 113.7, 111.0, 58.7, 32.9, 21.5; HRMS (APCI) calcd for $[C_{17}H_{19}NS_6]$ $[(M + H)^+]$ = 429.9914, found 429.9915. Anal. Calcd for $C_{17}H_{19}NS_6$: C, 47.51; H, 4.46; N, 3.26. Found: C, 47.44; H, 4.54; N, 3.02.

General Procedure for $\mathbf{1a}^{\bullet+}\mathbf{SbF_6}^--\mathbf{1d}^{\bullet+}\mathbf{SbF_6}^-$. The radical cation salts were prepared by one-electron oxidation in dichloromethane using 1 equiv of nitrosonium hexafluoroantimonate as the oxidant, and then the radical cation salts were obtained as precipitates by adding hexane to the solution. The purity was checked by elemental analysis.

ASSOCIATED CONTENT

Supporting Information

General methods, computational methods, ^{1}H and ^{13}C NMR spectra, UV−vis and UV−vis−NIR spectra, structures, energy profiles, angles and energies, and Cartesian coordinates and total energies of the optimized structures of all calculated molecules. This material is available free of charge via the Internet at http://pubs.acs.org.

AUTHOR INFORMATION

Corresponding Author

*T. Nishinaga. E-mail: nishinaga-tohru@tmu.ac.jp.

Notes

The authors declare no competing financial interest.

ACKNOWLEDGMENTS

This work was supported by a Grant-in-Aid for Scientific Research (B) (No. 22350021) from the Japan Society for the Promotion of Science (JSPS) and a Grant-in-Aid for Scientific Research on Innovative Areas (Stimuli-responsible Chemical Species for the Creation of Functional Molecules: No. 25109536) from the Ministry of Education, Culture, Sports, Science and Technology (MEXT).

REFERENCES

(1) (a) *Electronic Materials: The Oligomer Approach*; Müllen, K., Wegner, G., Eds.; WILEY-VCH Verlag: Hoboken, NJ, 1999. (b) Martin, R. E.; Diederich, F. *Angew. Chem., Int. Ed.* **1999**, *38*, 1350−1377. (c) Mishra, A.; Ma, C.-Q.; Bäuerle, P. *Chem. Rev.* **2009**, *109*, 1141−1276.

(2) Gronowitz, S.; Hörnfeldt, A.-B. *Thiophenes*; Elsevier: Oxford, U.K., 2004.

(3) Omastová, M.; Mičušík, M. *Chem. Pap.* **2012**, *66*, 392−414.

(4) van Haare, J. A. E. H.; Groenendaal, L.; Havinga, E. E.; Janssen, R. A. J.; Meijer, E. W. *Angew. Chem., Int. Ed.* **1996**, *35*, 638−640.

(5) Sessler, J. L.; Aguilar, A.; Sanchez-Garcia, D.; Seidel, D.; Köhler, T.; Arp, F.; Lynch, V. M. *Org. Lett.* **2005**, *7*, 1887−1890.

(6) (a) López-Pérez, A.; Robles-Machín, R.; Adrio, J.; Carretero, J. C. *Angew. Chem., Int. Ed.* **2007**, *46*, 9261−9264. (b) Robles-Machín, R.; López-Pérez, A.; González-Esguevillas, M.; Adrio, J.; Carretero, J. C. *Chem.—Eur. J.* **2010**, *16*, 9864−9873.

(7) (a) Niziurski-Mann, R. E.; Scordilis-Kelley, C.; Liu, T. L.; Cava, M. P.; Carlin, R. T. *J. Am. Chem. Soc.* **1993**, *115*, 887−891. (b) Parakka, J. P.; Cava, M. P. *Synth. Met.* **1995**, *68*, 275−279. (c) Kozaki, M.; Parakka, J. P.; Cava, M. P. *J. Org. Chem.* **1996**, *61*, 3657−3661. (d) Parakka, J. P.; Jeevarajan, J. A.; Jeevarajan, A. S.; Kispert, L. D.; Cava, M. P. *Adv. Mater.* **1996**, *8*, 54−59.

(8) (a) van Haare, J. A. E. H.; Groenendaal, L.; Peerlings, H. W. I.; Havinga, E. E.; Vekemans, J. A. J. M.; Janssen, R. A. J.; Meijer, E. W. *Chem. Mater.* **1995**, *7*, 1984−1989. (b) van Haare, J. A. E. H.; Groenendaal, L.; Havinga, E. E.; Meijer, E. W.; Janssen, R. A. J. *Synth. Met.* **1997**, *85*, 1091−1092.

(9) (a) Alemán, C.; Domingo, V. M.; Fajarí, L.; Juliá, L.; Karpfen, A. *J. Org. Chem.* **1998**, *63*, 1041−1048. (b) Domingo, V. M.; Alemán, C.; Brillas, E.; Juliá, L. *J. Org. Chem.* **2001**, *66*, 4058−4061.

(10) Audebert, P.; Catel, J.-M.; Le Coustumer, G.; Duchenet, V.; Hapiot, P. *J. Phys. Chem. B* **1998**, *102*, 8661−8669.

(11) Ogura, K.; Yanai, H.; Miokawa, M.; Akazome, M. *Tetrahedron Lett.* **1999**, *40*, 8887−8891.

(12) Nakazaki, J.; Chung, I.; Matsushita, M. M.; Sugawara, T.; Watanabe, R.; Izuoka, A.; Kawada, Y. *J. Mater. Chem.* **2003**, *13*, 1011−1022.

(13) Hansford, K. A.; Perez Guarin, S. A.; Skene, W. G.; Lubell, W. D. *J. Org. Chem.* **2005**, *70*, 7996−8000.

(14) Oliva, M. M.; Pappenfus, T. M.; Melby, J. H.; Schwaderer, K. M.; Johnson, J. C.; McGee, K.; da Silva Filho, D.; Bredas, J.-L.; Casado, J.; López Navarrete, J. T. *Chem.—Eur. J.* **2010**, *16*, 6866−6876.

(15) (a) Fujii, M.; Nishinaga, T.; Iyoda, M. *Tetrahedron Lett.* **2009**, *50*, 555−558. (b) Nishinaga, T.; Tateno, M.; Fujii, M.; Fujita, W.; Takase, M.; Iyoda, M. *Org. Lett.* **2010**, *12*, 5374−5377. (c) Nishinaga, T.; Miyata, T.; Tateno, M.; Koizumi, M.; Takase, M.; Iyoda, M.; Kobayashi, N.; Kunugi, Y. *J. Mater. Chem.* **2011**, *21*, 14959−14966.

(16) *Electropolymerization*; Cosnier, S., Karyakin, A., Eds.; WILEY-VCH Verlag: Hoboken, NJ, 2010.

(17) Rohde, D.; Dunsch, L.; Tabet, A.; Hartmann, H.; Fabian, J. *J. Phys. Chem. B* **2006**, *110*, 8223−8231.

(18) (a) Tabakovic, I.; Maki, T.; Miller, L. L.; Yu, Y. *Chem. Commun.* **1996**, 1911−1912. (b) Yu, Y.; Gunic, E.; Zinger, B.; Miller, L. L. *J. Am. Chem. Soc.* **1996**, *118*, 1013−1018.

(19) Merz, A.; Kronberger, J.; Dunsch, L.; Neudeck, A.; Petr, A.; Parkanyi, L. *Angew. Chem., Int. Ed.* **1999**, *38*, 1442−1446.

(20) (a) Hicks, R. G.; Nodwell, M. B. *J. Am. Chem. Soc.* **2000**, *122*, 6746−6753. (b) Casado, J.; Zgierski, M. Z.; Hicks, R. G.; Myles, D. J. T.; Viruela, P. M.; Ortí, E.; Ruiz Delgado, M. C.; Hernández, V.; López Navarrete, J. T. *J. Phys. Chem. A* **2005**, *109*, 11275−84.

(21) Lin, C.; Endo, T.; Takase, M.; Iyoda, M.; Nishinaga, T. *J. Am. Chem. Soc.* **2011**, *133*, 11339−11350.

(22) Hill, M. G.; Penneau, J. F.; Zinger, B.; Mann, K. R.; Miller, L. L. *Chem. Mater.* **1992**, *4*, 1106−1113.

(23) (a) Wakamiya, A.; Yamazaki, D.; Nishinaga, T.; Kitagawa, T.; Komatsu, K. *J. Org. Chem.* **2003**, *68*, 8305−8314. (b) Nishinaga, T.; Wakamiya, A.; Yamazaki, D.; Komatsu, K. *J. Am. Chem. Soc.* **2004**, *126*, 3163−3174. (c) Yamazaki, D.; Nishinaga, T.; Tanino, N.; Komatsu, K. *J. Am. Chem. Soc.* **2006**, *128*, 14470−14471.

(24) (a) Nishinaga, T.; Komatsu, K. *Org. Biomol. Chem.* **2005**, *3*, 561−569. (b) Komatsu, K.; Nishinaga, T. *Synlett* **2005**, 187−202.

(25) Miller, L. L.; Mann, K. R. *Acc. Chem. Res.* **1996**, *29*, 417−423.

(26) (a) Miller, J. S.; Novoa, J. J. *Acc. Chem. Res.* **2007**, *40*, 189−196. (b) Casado, J.; Burrezo, P. M.; Ramírez, F. J.; Navarrete, J. T. L.; Lapidus, S. H.; Stephens, P. W.; Vo, H.-L.; Miller, J. S.; Mota, F.; Novoa, J. J. *Angew. Chem., Int. Ed.* **2013**, *52*, 6421−6425.

(27) (a) Song, C.; Swager, T. M. *Org. Lett.* **2008**, *10*, 3575−3578. (b) Takita, R.; Song, C.; Swager, T. M. *Org. Lett.* **2008**, *10*, 5003−5005.

(28) (a) Trabolsi, A.; Khashab, N.; Fahrenbach, A. C.; Friedman, D. C.; Colvin, M. T.; Cotí, K. K.; Benítez, D.; Tkatchouk, E.; Olsen, J.-C.; Belowich, M. E.; Carmielli, R.; Khatib, H. A.; Goddard, W. A.; Wasielewski, M. R.; Stoddart, J. F. *Nat. Chem.* **2010**, *2*, 42−49. (b) Spruell, J. M.; Coskun, A.; Friedman, D. C.; Forgan, R. S.; Sarjeant, A. a.; Trabolsi, A.; Fahrenbach, A. C.; Barin, G.; Paxton, W. F.; Dey, S. K.; Olson, M. a.; Benítez, D.; Tkatchouk, E.; Colvin, M. T.; Carmielli, R.; Caldwell, S. T.; Rosair, G. M.; Hewage, S. G.; Duclairoir, F.; Seymour, J. L.; Slawin, A. M. Z.; Goddard, W. a.; Wasielewski, M. R.; Cooke, G.; Stoddart, J. F. *Nat. Chem.* **2010**, *2*, 870−879. (c) Barnes, J. C.; Fahrenbach, A. C.; Cao, D.; Dyar, S. M.; Frasconi, M.; Giesener, M. A.; Benítez, D.; Tkatchouk, E.; Chernyashevskyy, O.; Shin, W. H.; Li, H.; Sampath, S.; Stern, C. L.; Sarjeant, A. A.; Hartlieb, K. J.; Liu, Z.; Carmieli, R.; Botros, Y. Y.; Choi, J. W.; Slawin, A. M. Z.; Ketterson, J. B.; Wasielewski, M. R.; Goddard, W. A.; Stoddart, J. F. *Science* **2013**, *339*, 429−433.

(29) Iordache, A.; Oltean, M.; Milet, A.; Thomas, F.; Baptiste, B.; Saint-Aman, E.; Bucher, C. *J. Am. Chem. Soc.* **2012**, *134*, 2653−2671.

(30) Tateno, M.; Takase, M.; Iyoda, M.; Komatsu, K.; Nishinaga, T. *Chem.—Eur. J.* **2013**, *19*, 5457−5467 and referenced cited therein.

(31) Zhao, Y.; Truhlar, D. G. *Acc. Chem. Res.* **2008**, *41*, 157−167.

(32) Iyoda, M.; Otsuka, H.; Sato, K.; Nisato, N.; Oda, M. *Bull. Chem. Soc. Jpn.* **1990**, *63*, 80−87.

(33) Jana, G. H.; Jain, S.; Arora, S. K.; Sinha, N. *Bioorg. Med. Chem. Lett.* **2005**, *15*, 3592−3595.

(34) Miyata, Y.; Nishinaga, T.; Komatsu, K. *J. Org. Chem.* **2005**, *70*, 1147−1153.

(35) Hill, M. G.; Mann, K. R.; Miller, L. L.; Penneau, J.-F. *J. Am. Chem. Soc.* **1992**, *114*, 2728−2730.

(36) (a) Levillain, E.; Roncali, J. *J. Am. Chem. Soc.* **1999**, *121*, 8760−8765. (b) Raimundo, J.-M.; Levillain, E.; Gallego-Planas, N.; Roncali, J. *Electrochem. Commun.* **2000**, *2*, 211−215.

(37) The difference in the effects of the methoxy and methylthio substituents on the spin distribution of the radical cation precursor may also play some role. In $\mathbf{1c}^{\bullet+}$ and $\mathbf{1d}^{\bullet+}$, the Mulliken atomic spin densities on the O and S of the methoxy and methylthio substituents at the UM06-2X/6-31G(d) level in vacuo were 0.032 and 0.054, respectively. The larger spin delocalization into the S atom caused a smaller spin density on the neighboring C_β of thiophene ring in $\mathbf{1d}^{\bullet+}$ (0.100) than in $\mathbf{1c}^{\bullet+}$ (0.118) because of the plausible resonance structure shown below.

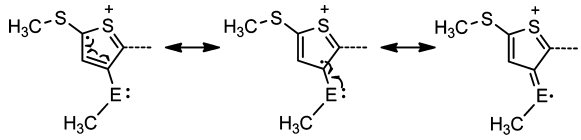

(38) Hoffmann, K. J.; Carlsen, P. H. J. *Synth. Commun.* **1999**, *29*, 1607−1610.

(39) Miller, L. L.; Yu, Y. *J. Org. Chem.* **1995**, *60*, 6813−6819.

(40) Taylor, E. C.; Vogel, D. E. *J. Org. Chem.* **1985**, *50*, 1002−1004.